Kütahya Dumlupınar University
Institute of Graduate Studies

Journal of Scientific
Reports-A
E-ISSN: 2687-6167
Number 52, March 2023

RESEARCH ARTICLE

INSIGHT INTO THE EFFECT OF TI/ZR OXIDE HYBRID PARTICLES ON DENTAL COMPOSITES: PARTICLE SYNTHESIS AND CHARACTERIZATION AND THE MECHANICAL BEHAVIOR OF COMPOSITES

Zerin YEŞİL ACAR[1*]

[1*]Burdur Mehmet Akif Ersoy University, Department of Dentistry Services, Vocational Schools, Burdur, zyacar@mehmetakif.edu.tr, ORCID: 0000-0002-1083-0222

Receive Date:11.12.2022 *Accepted Date: 10.03.2023*

ABSTRACT

Hybrid particles were synthesized with sol–gel-based hydrothermal method using alkoxide precursors, and the usability of these particles in dental composites was investigated. First, the effects of varying Ti/Zr and n_{acid}/ $n_{alkoxide}$ ratios on the crystal and microstructure of the synthesized particles (Ti, Zr) hybrids were investigated. X-ray diffraction (XRD), a particle size and a surface charge analyzer, thermogravimetric analysis (TGA), Brunauer–Emmett–Teller (BET) analysis, and Fourier transform infrared (FTIR) analysis were used to reveal the structural parameters. ZTit-1, ZTit-4, and ZTit-6 particles were crystalline, while ZTit-2, ZTit-3, and ZTit-5 particles were amorphous. The zeta potential of the most stable ZTit-4 particle was 43.33 mV. ZTit-3 particles had the highest surface area and ZTit-5 particles had the highest micropore area. The presence of Ti/Zr oxide and titanate structures was determined by FTIR analysis. In the next step of the study, the mechanical behavior of the synthesized Ti/Zr-based hybrid particles in the dental organic matrix was investigated. The flexural, compressive strengths, and microhardness of the ZTit-4 composite with optimal flowability were 175±16.1 MPa, 242±7.8 MPa, and 32.9 Hv.

Keywords: *ZrO_2–TiO_2, Mixed oxide, Sol–gel, Composite, Flowability, Microhardness.*

1. INTRODUCTION

Oral diseases negatively affect human health, well-being, and quality of life. Poor oral health linked to systemic bacterial and inflammatory sensitization can lead to adverse outcomes, including uncontrolled diabetes, cardiovascular disease, and respiratory disease [1]. A great majority of the world's population suffers from oral diseases, including caries, pulpitis, and periodontal disease, some of which can lead to defects in teeth and impaired function. Therefore, there is an urgent need for research on this subject. However, there is a significant challenge in rebuilding or reconstructing the heterogeneous and dynamic dental anatomical structure. To overcome these and similar problems, various dental materials are being studied and developed for use in reconstructing the curvature, color,

shape, and function of teeth [2]. An important particle used in materials studied and developed in dentistry is TiO_2. TiO_2 nanoparticles have been used to improve the fracture resistance of endodontically treated teeth, osseointegration of dental implants, antibacterial potential of a material, and adhesion to human teeth by incorporating them into adhesives [3]. Another important particle is ZrO_2, which is widely used in the production of dental prostheses, dental implants, and endodontic posts [3]. These applications have confirmed the potential use of TiO_2 and ZrO_2 nanoparticles in the development of materials used in the dental field.

TiO_2, a hard material with a high refractive index, is thermally stable, has superior mechanical properties, and is highly biocompatible. It exists in anatase, rutile, brookite (very rare), and amorphous forms [3,4]. ZrO_2 is naturally white, with high toughness, excellent strength, stable chemical properties, and good corrosion resistance, and is a biocompatible material that is a source of high-performance ceramic materials in terms of aesthetics and mechanical properties [2, 3, 5]. High-purity ZrO_2 exhibits three polymorphs depending on temperature: monoclinic, tetragonal, and cubic. Nanosized forms of TiO_2 and ZrO_2 particles, which are very popular in technological and scientific studies due to the aforementioned aspects, have recently been used more frequently in dental composites as they provide better dispersion, eliminate aggregation, and increase compatibility with organic polymers [6-8]. It was also reported that both ZrO_2 and TiO_2 nanoparticles are better than single additives due to the difference in the size of titanium and zirconium cations with the same stable oxidation state [6]. In the literature search, there are few studies in which TiO2 and ZrO2 particles are used together in dental composites, and the effects of these particles on the light transmittance and antibacterial effects of the composite were studied. There has been no discussion of the use of amorphous or crystalline TiZr hybrid oxides to strengthen the matrix.

With the continuous development of micro-/nanoscience and technology, it is possible to achieve practical functionalities such as desired mechanical properties, aesthetics, hardness, and fluidity (or viscosity) required for various clinical applications. Several factors, including the type of particle, its concentration by weight and volume, size, orientation, and distribution in the matrix, are critical in controlling the properties of designed dental composites. A strong matrix–particle interface is required to maximize the physical, mechanical, and biological performance of the resulting composites [9, 10].
The main aim in the present study was to synthesize particles using titanium and zirconium alkoxide precursors by polymeric sol–gel-based hydrothermal method and to investigate their usability in dental composites. On this basis, firstly, the effects of varying Ti/Zr and $n_{acid}/n_{alkoxide}$ ratios on the crystal structure and microstructure of hybrids of particles (Ti, Zr) with different crystallinity and content were investigated. The mechanical, flowability, and hardness behaviors of the synthesized pure ZrO_2, pure TiO_2 containing anatase–rutile crystal structures, and particles obtained in different phases including (Zr, Ti) oxide and (Zr, Ti) titanate in the dental matrix were determined.

2. MATERIAL AND METHOD

2.1. Chemicals and Apparatus

All chemicals were used at their commercially purchased purity without any purification. They comprised Zirconium (IV) n-propoxide (70 wt % in Propanol, Sigma-Aldrich, $Zr(OPr^n)_4$), Titanium (IV) isopropoxide (97 %, Sigma-Aldrich, $Ti(OPr^i)_4$) as alkoxide source, n-propanol (≥ 99.5 %, Sigma-

Aldrich, n-PrOH) as diluent/solvent, and hydrochloric acid (37 %, Sigma-Aldrich, HCl) as the catalyst. The crystalline phase was identified by Rigaku Geigerflex D Max/B model X-ray diffractometer. The size distribution and zeta potential of the particles were measured by a Malvern Zetasizer Nano series Nano-ZS model particle size analyzer. The alkoxide precursors remaining in the structure during the preparation of the particles were demonstrated using thermogravimetric analysis (TGA). An ASAP 2000 model Brunauer–Emmett–Teller (BET) analyzer was used to measure the surface of the particles. The change in the chemical structure of the synthesized particles was investigated by Fourier transform infrared (FTIR) spectroscopy (Perkin Elmer).

In the preparation of composites, camphorquinone (CQ) (Esschem) was chosen as a photoinitiator and ethyl 4-dimethyl amino benzoate (EDMAB) (Alfa Aesar) as a co-initiator. Nano-sized Aerosil 200 (12 nm, Evonik), micron-sized M8000 (1.8 µm, Sibelco), and synthesized zirconium and titanium-based hybrid oxide particles were used to form the inorganic phase. Silane-based 3-methacryloxy propyl trimethoxysilane (MPTS) (Aldrich) and n-hexane (Tekkim) were used respectively as the coupling agent and solvent to hold the organic matrix and inorganic particle together. The organic matrix was prepared using urethane dimethacrylate (UDMA) (Esschem). Bisphenol A ethoxylate dimethacrylate (BISEMA) (m+n=3, Esschem) was the main monomer. Triethylene glycol dimethacrylate (TEGDMA) (Esschem) was used both as a crosslinking and diluting monomer. Since the materials used in the dental field should have the properties required for clinical applications, the selection of composites was based on three-point flexural strength. In the testing and evaluation of the specimens according to the BS EN ISO 4049 standard, samples were first prepared in Teflon molds 25 mm in length, 2 mm in width, and 2 mm in thickness. After being placed in water, the samples were kept in an oven at 37±1 °C for 24 hours and dimensional measurements (length, width, and thickness) were recorded to an accuracy of 0.01 mm. The distance between the supports was adjusted according to the standard and a maximum charge (F) was applied to the sample at three points at a speed of 0.75 mm per minute until breakage. The results were calculated in mg/mm^3 using Equation 1.

$$\sigma = \frac{3xFxl}{2xbxh^2} \quad (1)$$

σ = Flexural strength, F = Maximum charge (N), L = Distance between supports (mm), b = Width (mm), h = Height (mm).

At least five samples were used to ensure meaningful and reliable test results. The three-point flexural strength values of the five samples were averaged and composites with average flexural strength values equal to or greater than 50 MPa were considered to have passed the test. According to clinical practice, composites must have compressive strength to resist intraoral forces (chewing) and flexural strength. For the testing and evaluation of the specimens, samples were prepared in Teflon molds 4 mm in thickness and 3 mm in diameter. A compressive force was applied to the sample from a single point perpendicularly at a rate of 0.5 mm/min until breakage. As a result of this force, the specimen fractured and the pressure applied at the moment of fracture was calculated in MPa. In order to ensure meaningful and reliable test results, at least five specimens were tested and the compressive strength values of the five tested specimens were averaged. Composites with average strength values equal to or greater than 100 MPa were considered to have passed the test. The surface hardness of the

JSR A
Journal of Scientific Reports

composites was measured using a Vickers microhardness tester with a loading of 50 grams for 10 seconds. Samples for microhardness measurement were prepared in the form of coins (2 mm thickness × 20 mm diameter) in Teflon molds. After soaking in distilled water at 37 °C for 1 day, the samples were tested. In order for the results to be reliable, measurements were taken by selecting three points at equal distances from the center of each specimen. The mean and standard deviation of the measurement results for each sample were calculated and used as the final result.

2.2. Methods

2.2.1. Preparation of particles

Particles with different crystallinity and content were prepared by varying the Ti/Zr and $n_{acid}/n_{alkoxide}$ ratios. The details of the synthesis conditions are given in Table 1 and the preparation of the particle named ZTit-1 is given as an example. Initially, 7.60 g of $Zr(OPr^n)_4$ was stirred in 100 ml of n-PrOH in a beaker until homogeneous. In another beaker, 1.43 g of $Ti(OPr^i)_4$ was dispersed in 70 ml of n-PrOH. The concentrated HCl calculated to give an $n_{acid}/n_{alkoxide}$ ratio of 0.464 was diluted in 4.389 ml of n-PrOH.

These two alkoxide sources dispersed in alcohol (molar Ti/Zr= 0.3) were brought together and diluted HCl was added dropwise. After acid addition, the alkoxide sol was transferred to the autoclave and placed in the hydrothermal unit at 250 °C. After the hydrothermal treatment, the autoclave cooled to room conditions and was removed from the unit. The resulting particles were centrifuged to precipitate and washed 3 times with n-PrOH. The particles were left to dry in a vacuum oven at 40 °C.

Table 1. Details of the synthesis conditions of the synthesized particles and naming of the samples.

Sample code	Ti/Zr ratio (mol)	Alcohol volume (ml)	Hydrothermal treatment (h)	Acid quantity (mol, 10^{-3})	$n_{acid}/n_{alkoxide}$ ratio
ZTit-1	0.3	180	12-14	9.74	0.46
ZTit-2	0.5	180	12-14	9.74	0.40
ZTit-3	0.8	180	12-14	9.74	0.33
ZTit-4	0.8	180	12-14	12.99	0.89
ZTit-5	1	180	12-14	9.74	0.30
ZTit-6	1	180	12-14	32.47	1.00

2.2.2. Preparation of composites

Modification of particle surfaces with coupling agents

In the modification of particle surfaces with silane-based coupling agents, all particle modifications were conducted in the same way, and the preparation of M8000 particles modified by 1.5% by weight is given as an example. After the MPTS required for the particle was placed in the container, n-hexane was added. In a separate container, diluted MPTS was added to the particle soaked in a certain amount of n-hexane with stirring. The particle–agent mixture was stirred at room conditions until the solvent evaporated. It was then dried at 60 °C to completely remove the solvent.

Preparation of composites containing particles modified with coupling agents

Composites were prepared by adding Nano-sized A200 particles and hybrid particles synthesized in half the amount by weight, provided that the ratio of micron-sized M8000 silica particles to the matrix was constant. In the studies on the preparation of composites, all mixtures were prepared in the same way, and the preparation of 15 g of composite containing (A200:ZTit-1):M8000 particle mixture with a composition of (1.00:1.00):4.44 at 40% and (UDMA:BISEMA3):TEGDMA monomer triplet with a composition of (80:10):10 at 60% is given as an example. First 0.045 g of CQ and 0.0225 g of EDMAB were completely dissolved in 0.9 g of TEGDMA. Then UDMA:BISEMA3 was added at a ratio of 8:1 and mixed in a mixer at 3600 rpm for 15 seconds. A mixture of 6.0 g of (A200:ZTit):M8000 particles was added to the prepared organic matrix. After the mixture was injected into the molds, light was applied for 20 seconds at the appropriate wavelength with a dental radiation probe. The effects of the synthesized zirconium- and titanium-based particles (ZTit-1 to ZTit-6) on the properties of the final product when added to the matrix with A200 at a ratio of 1:1 were investigated by a systematic approach (Figure 1). Detailed information on the particle contents of the prepared systems is given in Table 2.

Table 2. Coding of prepared composites and naming of nano- and micron-sized silica particles and synthesized hybrid particles used in the preparation of these composites.

Composite code	Nanosized particle (mod. ratio 5%)	Synthesized particle (mod. ratio 5%)	Micron-sized particle (mod. ratio 1.5%)
ZTit-0	A200	-	M8000
ZTit-1		ZTit-1	
ZTit-2		ZTit-2	
ZTit-3		ZTit-3	
ZTit-4		ZTit-4	
ZTit-5		ZTit-5	
ZTit-6		ZTit-6	

JSR A
Journal of Scientific Reports

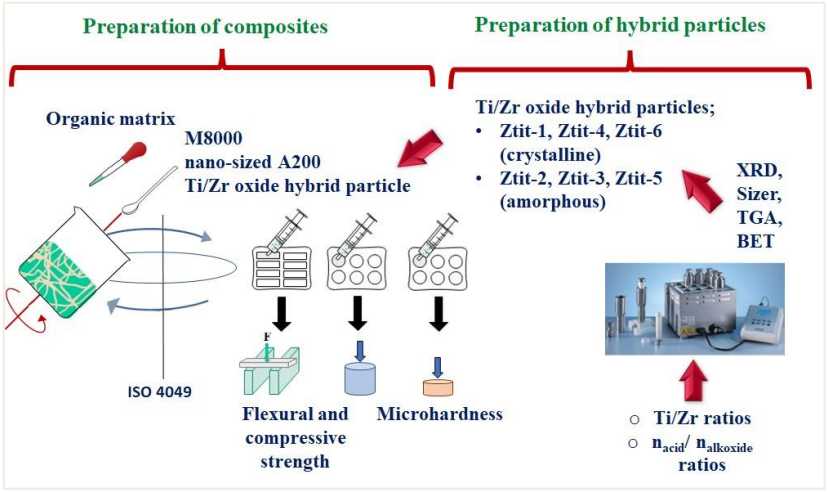

Figure 1. The experimental procedure of preparation of hybrid particles and composite.

3. RESULTS

Figure 2 and Figure 3 show the X-ray diffraction (XRD) patterns of the samples prepared by hydrothermal reaction at 250 °C for 12-14 h. Depending on the varying Ti/Zr and $n_{acid}/n_{alkoxide}$ ratios, nanoparticles in oxide form with different crystallinity and composition were obtained.

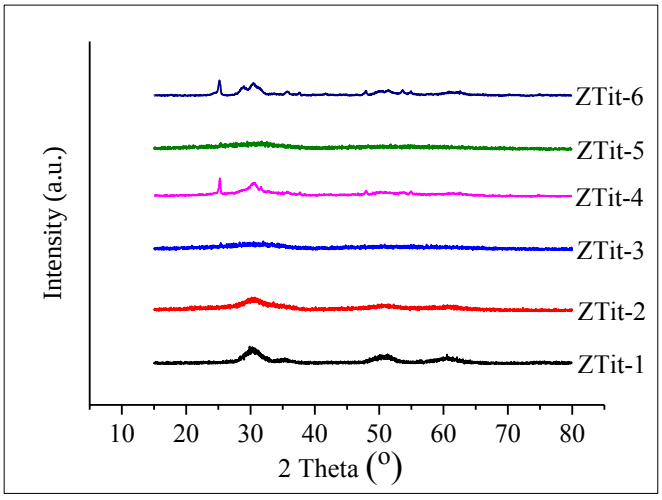

Figure 2. XRD patterns of synthesized zirconium- and titanium-based hybrid nanoparticles.

JSR A
Journal of Scientific Reports

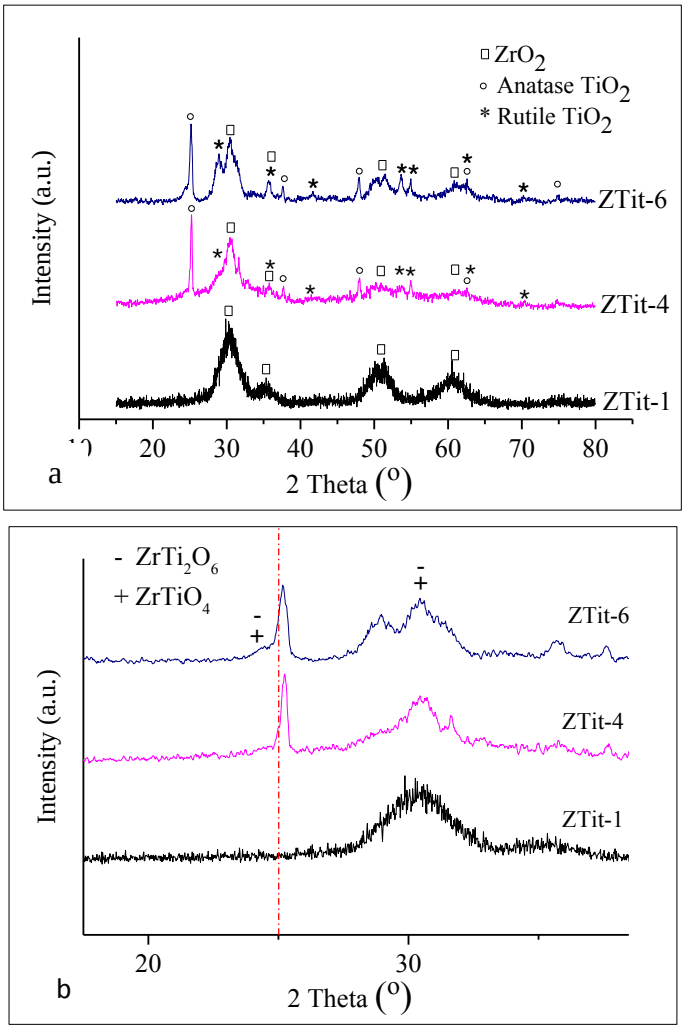

Figure 3. Characteristic XRD patterns of tetragonal ZrO_2, anatase, and rutile TiO_2 (a), triangular $ZrTi_2O_6$, and $ZrTiO_4$ species (b) in ZTit-1, ZTit-4, and ZTit-6 particles obtained in crystalline form.

The pattern seen at 2θ= 30.22, 35.53, 50.65, and 60.73 and corresponding to (011), (002), (112), (103) reflections of the ZTit-1 particle with a Ti/Zr ratio of 0.3 and $n_{acid}/n_{alkoxide}$ ratio of 0.46 indicates a pure tetragonal ZrO_2 (t-ZrO_2 JCPDS 80-0965) structure [11, 12]. When the reactivity behaviors of tetravalent alkoxides of zirconium and titanium transition metals were compared, a TiO_2 structure could not be formed at a low Ti/Zr ratio due to the higher reactivity of zirconium alkoxide. No crystalline phase was obtained in ZTit-2 or ZTit-3 structures with Ti/Zr ratios of 0.5 and 0.8, respectively [13]. This result is directly related to the low $n_{acid}/n_{alkoxide}$ ratio (0.400 and 0.333,

JSR A
Journal of Scientific Reports

respectively). It is thought that as the amount of acid, which plays a role in regulating the reaction rate and inorganic polymer network, decreases, the amount of water required for hydrolysis in the environment decreases, hydrolysis cannot be fully realized, and therefore crystal structures are not formed. This is supported by the formation of a crystalline structure in ZTit-4 particles obtained when the $n_{acid}/n_{alkoxide}$ ratio was increased from 0.333 to 0.89, provided that the Ti/Zr ratio remained constant at 0.8. When the reflections corresponding to 2θ angles in the pattern of ZTit-4 particles are examined comparatively, it is seen that ZrO_2 and anatase/rutile TiO_2 phases with a tetragonal crystal structure were formed. The patterns corresponding to the reflection at 2θ= 25.25 (101) and 2θ= 27.42 (110) were the main peaks of the anatase and rutile TiO_2 phases, respectively. The estimated anatase/rutile ratio was calculated based on the main peaks using the Spurr–Myers equation [14]:

$$X_A(\%) = \frac{100}{(1+1.265*\frac{I_R}{I_A})} \quad (2)$$

$$X_R(\%) = \frac{100}{(1+0.8*\frac{I_A}{I_R})} \quad (3)$$

Here, I_A is the anatase phase density at 2θ= 25.25, I_R is the rutile phase density at 2θ= 27.42, and X_R and X_A are the weight percentages of anatase and rutile phases in the sample. Using Equations 2 and 3 in the XRD spectrum of the mixed phase, it was determined that the crystal structure contains 53% anatase and 47% rutile.

When the patterns of ZTit-5 and ZTit-6 particles obtained when working with low (0.30) and high (1.00) acid amounts with a Ti/Zr ratio of 1.0 were examined, results similar to those from ZTit-3 and ZTit-4 were obtained. In the case of insufficient acid content, the ZTit-5 particle remained in the crystalline phase, while in the ZTit-6 sample prepared by increasing the acid content, tetragonal ZrO_2, anatase/rutile TiO_2 structure, orthorhombic $ZrTi_2O_6$, and $ZrTiO_4$ phases were observed. The characteristic XRD peaks at 2θ= 24.87 and 2θ= 24.71 indicate the $ZrTi_2O_6$, and $ZrTiO_4$ phase in the hybrid particle. Reflections of the pure tetragonal ZrO_2 structure are given in Figure 2a. Moreover, XRD peaks at 2θ= 25.24 (101) and 2θ= 47.79 (101) indicate the presence of the anatase phase, while peaks at 2θ= 27.42 (110) and 2θ= 54.5 indicate rutile formation. According to the Spurr–Meyers equation, the crystal structure contains 78% anatase and 21% rutile by weight.

The dispersion behavior of the synthesized zirconium- and titanium-based hybrid nanoparticles is given in Figure 4.

JSR A
Journal of Scientific Reports

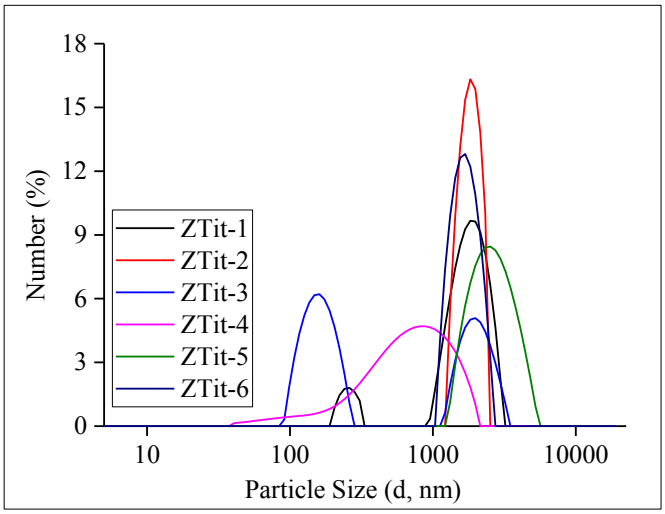

Figure 4. Particle size distributions of synthesized zirconium- and titanium-based hybrid nanoparticles.

ZTit-1 and ZTit-3 particles have bimodal distributions, while ZTit-2, ZTit-4, ZTit-5, and ZTit-6 particles have monomodal distributions. Except for ZTit-4, these synthesized hybrid particles exhibited a monodisperse distribution. Recent studies show that polydispersity characterization has become essential in nanoparticle applications, because it is difficult to control homogeneity in the size distribution of the sample and aggregation of nanoparticles is often a possible behavior [15]. ZTit-1 with the lowest titanium alkoxide ratio (low $n_{acid}/n_{alkoxide}$ ratio) exhibited an increasing bimodal distribution in parallel with the increase in the condensation reaction. At low acid and hence water contents, hydrolysis is slower than condensation and the excess of zirconium alkoxide in the solvent promotes the development of Zr-O-Zr chains through alcoholization, resulting in the formation of particles with relatively large sizes [16]. In ZTit-4 obtained by increasing the amount of titanium precursor (Ti/Zr= 0.8), the expected formation of larger polydisperse crystallites took place, as more alkoxide was available for growth on each crystal after nucleation. They exhibited monomodal and monodisperse distribution in high acid ZTit-6 with a Ti/Zr ratio of 1.0. A larger amount of water suppresses the growth of Zr-O-Zr chains by oxolation, resulting in smaller particles. An increase in the amount of water leads to an increase in the number of n in Zr(OH)n formation, resulting in the formation of more reactive species that can contribute to the development of new species. The formation of the Zr-O-Zr network proceeds through olation and leads to even larger particles [16]. As a result, increasing the acid content of the medium in the synthesis of ZTit-6, which exhibits a slightly narrower particle size distribution, led to the formation of finer crystallites, which is in qualitative agreement with the reports of supporting studies [17].

Zeta potential values, which give information about the distribution of hybrid particles obtained at different alkoxide and acid ratios in a solvent, are presented in Table 3.

JSR A
Journal of Scientific Reports

Table 3. Zeta potentials of synthesized zirconium- and titanium-based hybrid nanoparticles.

Sample Code	Zeta Potential (mV)
ZTiT-1	13.97
ZTiT-2	18.91
ZTiT-3	31.02
ZTiT-4	43.33
ZTiT-5	6.60
ZTiT-6	8.29

The synthesized hybrid particles may have -OH functional groups on their surfaces that are not incorporated into the metal oxide network, resulting in a positive surface charge. The surface charge of ZTit-4 particles dominated by the TiO_2 crystalline phase is high compared to the others, with a high positive zeta potential value (≥30 mV) indicating high stability. Dispersions of ZTit-3 and ZTit-4 particles in water with zeta potentials ≥30 mV are stable due to the dominant repulsive forces. In the structures where ZrO_2 and its derivative crystal phases are formed (ZTit-1, ZTit-5, and ZTit-6), the surface charges are low. The variation in particle surface charges depending on the reaction kinetics requires further investigation. As a result, during the synthesis, the difference in the Ti/Zr and $n_{acid}/n_{alkoxide}$ ratios not only led to amorphous and crystalline particles, but these variables also led to differences in the positive surface charges of the final structure.

TGA thermograms of particles obtained at different Ti/Zr and $n_{acid}/n_{alkoxide}$ ratios are given in Figure 5.

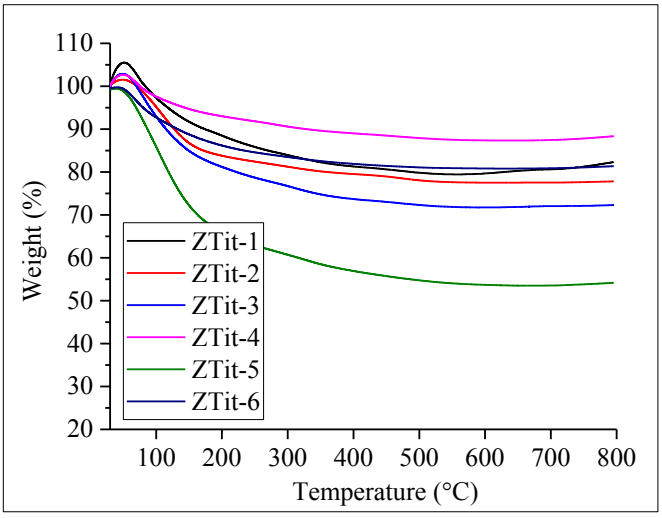

Figure 5. TGA thermogram of synthesized zirconium- and titanium-based hybrid nanoparticles.

JSR A
Journal of Scientific Reports

The first noticeable feature in the thermograms is the higher mass losses in the amorphous ZTit-2, ZTit-3, and ZTit-5 structures that failed to transition to the crystalline phase. This is directly related to the increasing amount of alkoxide precursors that remain in the structure without participating in hydrolysis/condensation reactions due to the low $n_{acid}/n_{alkoxide}$ ratio. The aggressive loss from 70 to 150 °C is due to water and solvent remaining in the particle pores. The relatively gentle second curve from 200 to 400 °C is due to the removal of alkoxides.

The BET surface area, micropore area and external surface area, and micropore volume values of the synthesized nanoparticles differing according to the varying Ti/Zr and $n_{acid}/n_{alkoxide}$ ratios are given in Table 4.

Table 4. BET surface area, micropore area and external surface area, and micropore volume values.

	BET surface area (m^2/g)	Micropore area (A, m^2/g)	External surface area (mesopore area) (B, m^2/g)	A/B	Micropore volume (cm^3/g), 10^{-2}
ZTit-1	60.21	57.99	2.22	26.12	2.99
ZTit-2	172.98	98.70	74.28	1.33	5.18
ZTit-3	310.37	183.89	126.48	1.45	9.83
ZTit-4	155.48	-32.71	188.19	-	-1.97
ZTit-5	288.76	206.34	82.42	2.50	10.71
ZTit-6	74.17	-8.41	82.58	-	-0.52

The BET results show that ZTit-3 and ZTit-5 had the highest surface areas. In general, ZTit-2, ZTit-3, and ZTit-5 with amorphous structures were found to have high surface areas compared to the others. The surface areas of crystalline ZTit-1, ZTit-4, and ZTit-6 particles were lower. Negative micropore area and volume values were observed for ZTit-4 and ZTit-6 particles. This was due to the inadequacy of the t-plot equation for calculating pore size and other related properties in microporous and/or mesoporous structures [18].

The FTIR spectra of the particles obtained at different Ti/Zr and $n_{acid}/n_{alkoxide}$ ratios in the wavelength range from 4000 cm^{-1} to 400 cm^{-1} are given in Figures 6a-6b.

JSR A
Journal of Scientific Reports

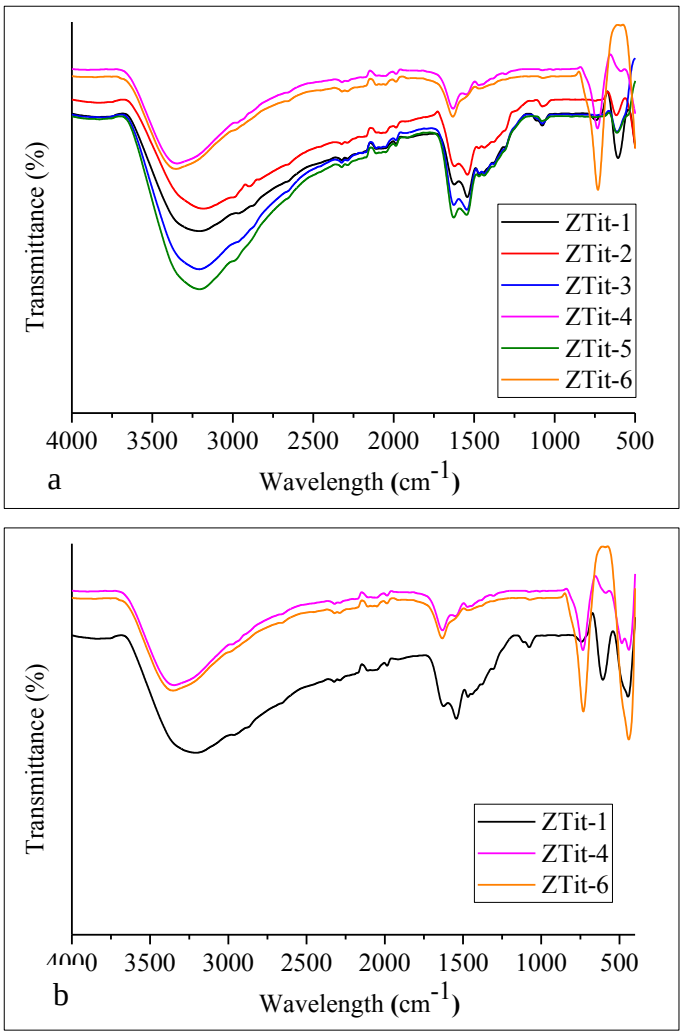

Figure 6. FTIR spectrum of synthesized zirconium- and titanium-based hybrid nanoparticles (a), magnified FTIR spectrum of particles obtained in crystalline form (b).

The broad absorption band around 3400 cm^{-1} in the FTIR spectrum in Figure 4a corresponds to -OH stretching vibrations indicating the presence of molecular water in the structure. The spectrum of ZTit-1 shows characteristic bands localized at approximately 1540 cm^{-1} and 450 cm^{-1}. These bands overlap with the reflections of the tetragonal ZrO_2 particle ([19, 20]. The peaks and bands seen in the FTIR spectrum of the ZTit-4 particle are consistent with the data reported in the literature for anatase and rutile crystal forms. The reported data show that the broad and intense bands at 520 cm^{-1} and between 900 and 400 cm^{-1} pertain to Ti-O stretching and bending vibrations in the anatase crystal

JSR A
Journal of Scientific Reports

phase [21, 22]. The peaks at 464 cm^{-1} and 530 cm^{-1} are characteristic stretching vibrations of the Ti-O-Ti network in anatase TiO_2 [23]. When the fingerprint region of ZTit-4 is observed in more detail in Figure 4b, it is seen that the peaks and bands overlap with the peaks of pure ZrO_2 and anatase and rutile TiO_2 phases. The observed shifts are within acceptable limits for the interpretation of FTIR spectra. As seen in Figure 4-b, the stretching and bending vibrations of the Ti-O bond appeared at 593 cm^{-1} and the characteristic stretching vibration of the Ti-O-Ti network appeared at 485 cm^{-1}. The FTIR spectrum of the rutile form of TiO_2 is largely similar to that of anatase. For the particle in question, the maximum band at 680 cm^{-1} and the intense band at 536 cm^{-1} in the range of 830-400 cm^{-1} are specific to the pure rutile Ti-O vibration with a high transmittance value [21]. The stresses of this vibration are seen at around 736 cm^{-1} and 593 cm^{-1} in the spectrum. According to the studies in the literature, in the FTIR spectrum of the anatase/rutile mixture, the maximum of the main band due to the vibrations of Ti-O bonds and the Ti-O-Ti network is expected to be in the 576 cm^{-1} range [21]. The peak at 593 cm^{-1} in the spectrum of the synthesized ZTit-4 particle is the maximum of the main band. In the spectrum of ZTit-6, vibrational peaks pertaining to anatase TiO_2, rutile TiO_2, and tetragonal ZrO_2 were observed and these are consistent with the literature. Peaks between 500 cm^{-1} and 710 cm^{-1} are related to Ti-O and Zr-O-Ti vibrations [24].

In order to provide both aesthetic and mechanical properties such as translucency, antibacterial, flowability, biocompatability and opacity in dental composites, particles with different ratios and sizes by weight are doped [10, 25]. Accordingly, composites were prepared by adding the synthesized hybrid particles with varying Ti/Zr and $n_{acid}/n_{alkoxide}$ ratios into the organic matrix with a replacement of 50% of A200. Of these particles; ZTit-1, ZTit-4, and ZTit-6 particles were crystalline, while ZTit-2, ZTit-3, and ZTit-5 particles were amorphous. Yield behavior is considered the main feature in evaluating the usability of dental composites developed for clinical applications [26]. The yield behavior of composites doped with TiO_2-ZrO_2 mixed oxides with different crystalline phases and the change in flexural strengths are given in Figure 7.

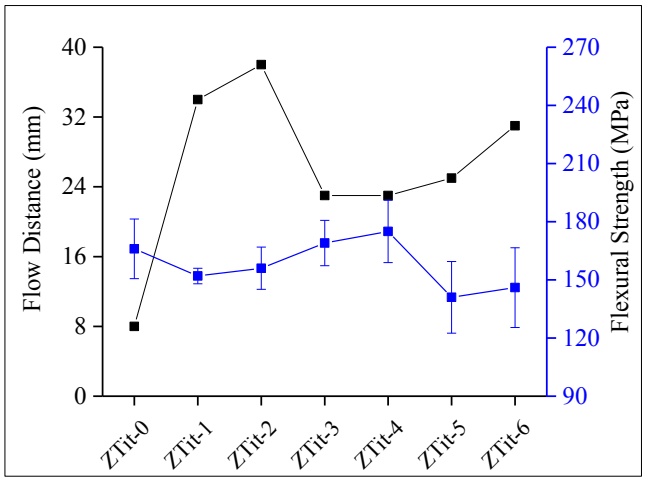

Figure 7. Flow distance and flexural strength graph of composites prepared by using hybrid particles.

The yield values of the composites were higher compared to those of ZTit-0 without hybrid particles. This was directly related to the larger particle size of amorphous and crystalline ZTit particles compared to A200. Due to their low surface area/volume ratio, the volume of the organic matrix per unit area in the composite was higher [27, 28]. The yield behavior of the crystal particles was ZTit-1>ZTit-6>ZTit-4 with yield distances of 34 mm, 31 mm, and 23 mm, respectively. The flowability of the composites in which they were used varied due to the fact that the three particles were modified with a constant amount of coupling agent without regard to their size-dependent surface areas. Mechanical characterization is an important phenomenon in the development of dental composite materials. Inorganic filler particles have a significant effect on the mechanical characterization of dental composite materials. In general, the strengthening of inorganic filler particles can be attributed to two aspects: (i) the binding force between the dental polymer matrix and inorganic particles, the interface, and (ii) the particle size distribution [29]. The flexural strengths of composites containing crystalline particles exhibited behavior of ZTit-4>ZTit-1>ZTit-6. The highest flexural strength value belonged to the ZTit-4 composite (175±16.1 MPa) and a significant increase was observed compared to the ZTit-0 composite: 166±15.4 MPa. This result is directly related to its lower flowability compared to ZTit-1 and ZTit-6. Optimal flowability in the molding of composites prevents undesirable conditions such as air bubbles that can cause microcracks in the structure. The flexural strengths of the more flowable ZTit-1 and ZTit-6 composites were 152±4.0 MPa and 146±20.6 MPa. According to the pure system, the decrease in strength is directly related to the composites moving away from optimal flowability. Composites using amorphous ZTit-2, ZTit-3, and ZTit-5 particles did not show a linear change at a low $n_{acid}/n_{alkoxide}$ ratio. With increasing alkoxide, their flowabilities decreased from 38 mm to 23 mm. ZTit-3 with the lowest flowability showed a strength of 169±11.7 MPa, while ZTit-5 composite with almost similar flowability showed a strength of 141±18.5 MPa. This result is closely related to the surface charges of the particles. The homogeneous distribution of the ZTit-3 particle with 31.01 mV zeta potential in the matrix resulted in an improvement in flexural strength. The surface charge-dependent zeta potential of the ZTit-5 particle of similar flowability was 6.59 mV, which did not exhibit a homogeneous distribution in the matrix and negatively affected the flexural strength.

A compressive strength test was used in laboratory experiments to simulate the chewing forces that stress composites used in the dental field [6]. The change in compressive strength versus yield behavior of composites containing the synthesized hybrid particles is shown in Figure 8.

JSR A
Journal of Scientific Reports

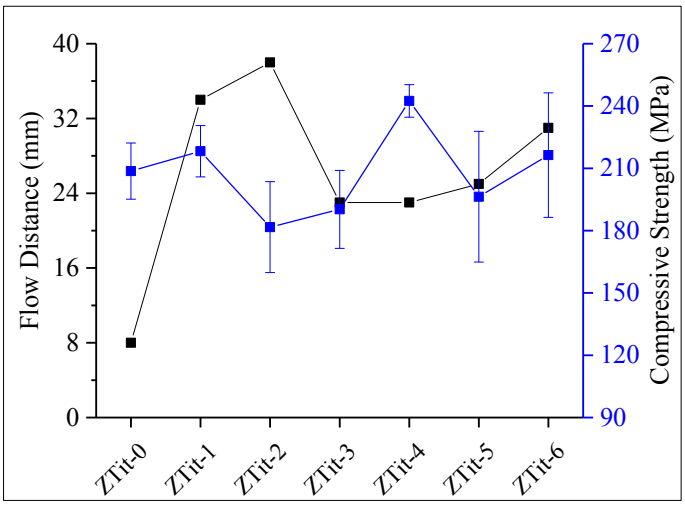

Figure 8. Flow distance and compressive strength graph of composites prepared using hybrid particles.

The compressive strength of the composites using hybrid particles did not exhibit a linear change compared to the pure composite. The compressive strengths of composites containing crystalline ZTit-1, ZTit-4, and ZTit-6 particles were 218±12.3 MPa, 242±7.8 MPa, and 218±29.9 MPa, respectively. Their compressive strength was higher compared to that of the pure ZTit-0 composite (208±13.5 MPa). Due to the optimal surface charge and homogeneous distribution of ZTit-4 particles in the matrix, the composite obtained with optimal flowability exhibited the highest strength. While the compressive strength values of the ZTit-1 and ZTit-6 composites based on their close flowability were similar, their standard deviation varied. This difference in standard deviation arose from the surface charges affecting their distribution in the matrix. The standard deviation of the compressive strength of ZTit-1, which had a slightly more positive surface charge, was lower, as expected. The flowability of the composites using amorphous ZTit-2, ZTit-3, and ZTit-5 particles decreased at a low $n_{acid}/n_{alkoxide}$ rate. The compressive strengths were 181±21.9 MPa, 190±18.8 MPa, and 196±31.4 MPa, respectively. The optimal system in terms of flowability and zeta potential was the composite prepared with ZTit-3 particles and the standard deviation in compressive strength was slightly lower than the others. The standard deviation of the ZTit-6 composite, which exhibited the highest compressive strength, was also quite high. This result shows the importance of composite flowability and particle surface charge as a factor in particle distribution in the matrix. It is also evidence that they may be in competition.

Another test that provides information about the mechanical properties of the material is the microhardness test. The clinical significance of hardness is related to aesthetic restorations (discoloration and erosion), medical consequences of periodontal disease, and the development of secondary caries due to increased plaque accumulation [30]. This behavior of the composite can be

influenced by monomer type, filler type, morphology, volume, and weight. In particular, the type and size of inorganic particles and the extent of particle loading can lead to significant differences in the microhardness of these materials [31]. On this basis, the change in the microhardness values of the synthesized composites containing hybrid particles of different crystallinity and microstructure is shown in Figure 9.

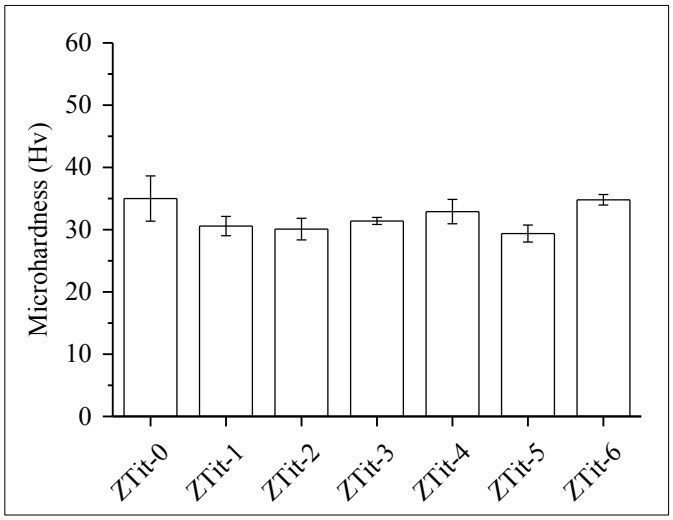

Figure 9. Microhardness graph of composites prepared using synthesized hybrid particles.

When the microhardness of the composites was analyzed, the microhardness of all composites except ZTit-2 was lower compared to ZTit-0. This decrease was related to the decrease in surface area due to increasing particle size. An important parameter affecting the microhardness of composites is the distribution of particles in the matrix. Therefore, as the particle size increases, the amount of particles per unit area loaded into the matrix decreases, leading to the formation of inter-particle voids. This results in a decrease in surface resistance to the notch created in the composite surface for hardness measurement [32, 33]. The microhardness of the composites using hybrid particles with the crystalline structure was analyzed and the decrease in the microhardness values of the composites containing ZTit-4 and ZTit-6 was less compared to ZTit-1. The formation of hybrid (Zr, Ti) and oxide structures during the synthesis of ZTit-4 and ZTit-6 particles enabled them to be obtained in smaller sizes. This resulted in higher microhardness values in the composites in which they were doped [32].

4. CONCLUSION AND COMMENT

In order to obtain high purity and more homogeneous titanium and/or zirconium oxide particles, a solvent-based wet chemical synthesis method has been developed as an alternative to the traditional solid-state reaction route. Within the scope of the method, the variation in Ti/Zr and $n_{acid}/n_{alkoxide}$ ratios resulted in particles with different crystal phases and microstructures. The most important conclusion

based on the synthesis/characterization of the particles was that by improving the synthesis conditions of the particles obtained in amorphous form (increasing the amount of acid, increasing the synthesis temperature) transition to the crystalline form with optional composition can be achieved. Accordingly, particle sizes, surface charges, and the presence/amount of alkoxide precursors that may remain in the structure can be controlled. Another important aspect of the study was to investigate the behavior of the synthesized Ti/Zr-based hybrid particles in the selected dental organic matrix. The flexural, compressive strengths, and microhardness of the composite containing ZTit-4 particles with optimal flowability were 175±16.1 MPa, 242±7.8 MPa, and 32.9 Hv, respectively. As a result, the mechanical behavior of the dental composite is influenced by the type, size, weight/volume, and surface properties of the particles forming the filler phase.

ACKNOWLEDGMENTS

I would like to thank Prof. Dr. Meltem ASİLTÜRK for allowing me to benefit from the laboratory facilities.

AUTHOR STATEMENT

Zerin YEŞİL ACAR: Methodology, Investigation, Original Draft Writing, Review and Editing

CONFLICT OF INTEREST

As the authors of this study, we declare that we do not have any conflict of interest statement.

ETHICS COMMITTEE APPROVAL AND INFORMED CONSENT

As the author of this study, we declare that we do not have any ethics committee approval and/or informed consent statement.

REFERENCES

[1] Aminoroaya, A., Neisiany, R.E., Khorasani, S.N., Panahi, P., Das, O., Madry, H., Cucchiarini, M., Ramakrishna, S., (2021), A review of dental composites: Challenges, chemistry aspects, filler influences, and future insights, Composites Part B: Engineering, 216, 108852.

[2] Hu, C., Sun, J., Long, C., Wu, L., Zhou, C., Zhang, X., (2019), Synthesis of nano zirconium oxide and its application in dentistry, Nanotechnology Reviews, 8(1), 396-404.

[3] Al-Saleh, S., Alateeq, A., Alshaya, A.H., Al-Qahtani, A.S., Tulbah, H.I., Binhasan, M., Shabib, S., Farooq, I., Vohra, F., Abduljabbar, T., (2021), Influence of TiO_2 and ZrO_2 nanoparticles on adhesive bond strength and viscosity of dentin polymer: A physical and chemical evaluation, Polymers, 13(21), 3794.

[4] Haas, K., Azhar, G., Wood, D.J., Moharamzadeh, K., Van Noort, R., (2017), The effects of different opacifiers on the translucency of experimental dental composite resins, Dental Materials, 33(8), e310-e316.

[5] Hafızoğlu, M.A., Boyraz, T., Akkuş, A., The effect of mullite addition on wear properties of titania doped zirconia ceramics, Dicle Üniversitesi Mühendislik Fakültesi Mühendislik Dergisi, 13(1), 43-50.

[6] Felemban, N.H., Ebrahim, M.I., (2017), The influence of adding modified zirconium oxide-titanium dioxide nano-particles on mechanical properties of orthodontic adhesive: an in vitro study, BMC Oral Health, 17(1) 1-8.

[7] Sakhno, O. , Goldenberg, L., Stumpe, J., Smirnova, T., (2007), Surface modified ZrO2 and TiO2 nanoparticles embedded in organic photopolymers for highly effective and UV-stable volume holograms, Nanotechnology, 18(10), 105704.

[8] Cazan, C., Enesca, A., Andronic, L., (2021), Synergic effect of TiO2 filler on the mechanical properties of polymer nanocomposites, Polymers, 13(12), 2017.

[9] Fu, S.-Y., Feng, X.-Q., Lauke, B., Mai, Y.-W., (2008), Effects of particle size, particle/matrix interface adhesion and particle loading on mechanical properties of particulate–polymer composites, Composites Part B: Engineering, 39(6), 933-961.

[10] Cho, K., Rajan, G., Farrar, P., Prentice, L., Prusty, B.G., (2022), Dental resin composites: A review on materials to product realizations, Composites Part B: Engineering, 230, 109495.

[11] Wang, J., Yin, W., He, X., Wang, Q., Guo, M., Chen, S., (2016), Good biocompatibility and sintering properties of zirconia nanoparticles synthesized via vapor-phase hydrolysis, Scientific reports, 6(1), 1-9.

[12] Li, W., Zhao, Z., (2016), Hierarchically structured tetragonal zirconia as a promising support for robust Ni based catalysts for dry reforming of methane, RSC advances, 6(77), 72942-72951.

[13] Tran, T.T.H., Bui, T.T.H., Nguyen, T.L, Man, H.N., Tran, T.K.C., (2019), Phase-pure brookite TiO2 as a highly active photocatalyst for the degradation of pharmaceutical pollutants, Journal of Electronic Materials, 48(12), 7846-7861.

[14] El-Sherbiny, S., Morsy, F., Samir, M., Fouad, O.A., (2014), Synthesis, characterization and application of TiO2 nanopowders as special paper coating pigment, Applied Nanoscience, 4(3), 305-313.

[15] Clayton, K.N., Salameh, J.W., Wereley, S.T., Kinzer-Ursem, T.L., (2016), Physical characterization of nanoparticle size and surface modification using particle scattering diffusometry, Biomicrofluidics, 10(5), 054107.

[16] Marchisio, D.L., Omegna, F., Barresi, A.A., Bowen, P., (2008), Effect of mixing and other operating parameters in sol− gel processes, Industrial & engineering chemistry research, 47(19), 7202-7210.

[17] Wahi, R.K., Liu, Y., Falkner, J.C., Colvin, V.L., (2006), Solvothermal synthesis and characterization of anatase TiO_2 nanocrystals with ultrahigh surface area, Journal of colloid and interface science, 302(2), 530-536.

[18] Galarneau, A., Mehlhorn, D., Guenneau, F., Coasne, B., Villemot, F., Minoux, D., Aquino, C., Dath, J.-P., (2018), Specific surface area determination for microporous/mesoporous materials: The case of mesoporous FAU-Y zeolites, Langmuir, 34(47), 14134-14142.

[19] Bermúdez-Reyes, B., Contreras-García, M., Almaral-Sánchez, J., Espitia-Cabrera, I., Espinoza-Beltrán, F., (2012), Chemical anchorage of Hydroxyapatite on 316LSS using a ZrO2 interlayer for orthopedic prosthesis applications, Superficies y vacío, 25(3), 150-156.

[20] Chandradass, J., Balasubramanian, M., Hyeon Kim, K., (2011), Solution phase synthesis of t-ZrO2 nanoparticles in ZrO2–SiO2 mixed oxide, Journal of Experimental Nanoscience, 6(1), 38-48.

[21] Johnson, M.S., Ates, M., Arslan, Z., Farah, I.O., Bogatu, C., (2017), Assessment of crystal morphology on uptake, particle dissolution, and toxicity of nanoscale titanium dioxide on Artemia salina, Journal of Nanotoxicology and Nanomedicine , 2(1), 11-27.

[22] Al-Taweel, S.S., Saud, H.R., (2016), New route for synthesis of pure anatase TiO2 nanoparticles via utrasound-assisted sol-gel method, J. Chem. Pharm. Res, 8(2), 620-626.

[23] Liu, K., Zhu, L., Jiang, T., Sun, Y., Li, H., Wang, D., (2012), Mesoporous micro-nanometer composite structure: synthesis, optoelectric properties, and photocatalytic selectivity, International Journal of Photoenergy, 2012.

[24] Bavya Devi, K., Singh, K., Rajendran, N., (2011), Sol–gel synthesis and characterisation of nanoporous zirconium titanate coated on 316L SS for biomedical applications, Journal of sol-gel science and technology, 59(3), 513-520.

[25] Elfakhri, F., Alkahtani, R., Li, C., Khaliq, J., (2022), Influence of filler characteristics on the performance of dental composites: A comprehensive review, Ceramics International.

[26] Baroudi, K., Rodrigues, J.C., (2015), Flowable resin composites: a systematic review and clinical considerations, Journal of clinical and diagnostic research, 9(6), ZE18.

[27] Wang, Y., (2007), High elastic modulus nanopowder reinforced resin composites for dental applications, University of Maryland, College Park.

[28] Özak, Ş., (2012), Farkli yapıdaki yapay dişlerin mikrosertlik, yüzey pürüzlülüğü ve renk stabilitesi üzerinde değişik sıvı ortamlarının etkisinin değerlendirilmesi, Ankara Üniversitesi Sağlık Bilimleri Enstitüsü, Doktora tezi.

[29] Yadav, R., Meena, A., (2022), Effect of aluminium oxide, titanium oxide, hydroxyapatite filled dental restorative composite materials on physico-mechanical properties, Ceramics International, 48(14), 20306-20314.

[30] Gurbuz, O., Cilingir, A., Dikmen, B., Özsoy, A., Meltem, M., (2020), Effect of surface sealant on the surface roughness of different composites and evaluation of their microhardness, European oral research, 54(1), 1-8.

[31] Atabek, D., Bani, M., Öztaş, N., Ekçi, E.S., (2016), The effect of various polishing systems on the surface roughness of composite resins, Acta Odontologica Turcica, 33(2).

[32] El-Nagar, H., El-sadek, A., Ezzeldien, M., (2020), Structural analysis, optical and mechanical properties of $Ti_xZr_{1-x}O_2$ nanoparticles synthesized by modified co-precipitation route, Applied Physics A, 126(2), 1-12.

[33] Alrahlah, A., Khan, R., Vohra, F., Alqahtani, I.M., Alruhaymi, A.A., Haider, S., Al-Odayni, A.-B., Saeed, W.S., Murthy, H., Bautista, L.S., (2022), Influence of the Physical Inclusion of ZrO_2/TiO_2 Nanoparticles on Physical, Mechanical, and Morphological Characteristics of PMMA-Based Interim Restorative Material, BioMed Research International 2022.